IJCRT.ORG ISSN : 2320-2882

INTERNATIONAL JOURNAL OF CREATIVE RESEARCH THOUGHTS (IJCRT)

An International Open Access, Peer-reviewed, Refereed Journal

Allantoin: A Comprehensive Review of Mechanism And Laboratory Methods.

1Mr. Siddhant S. Rathod, 2Dr. Rajesh Z. Mujariya

1M.pharm Student, 2Principal And Director

1Institute of Pharmaceutical Science And Research (IPSR),

2Institute of Pharmaceutical Science And Research (IPSR)

Abstract:- The hydrogels represent by the three-dimensional networks comprising physically or chemically interconnected bonds of hydrophilic polymers. These insoluble hydrophilic structures possess the ability to absorb fluids from wounds and facilitate the diffusion of oxygen, thereby expediting the healing process. The primary objective of this current research is to create and assess a hydrogel containing Neomycin sulfate, intended for enhancing wound healing. Neomycin sulfate, an antibiotic employed in the treatment of bacterial skin infections, has proven efficacy in addressing infected lacerations, wounds, torn tissue, fatigue, and minor burns. The hydrogel formulation of neomycin sulfate, designed for topical application to promote wound healing, was developed using guar gum and Carbopol-940, followed by comprehensive evaluations.

Keywords: Hydrogel, Allantoin, aloevera, Topical Delivery System

INTRODUCTION

Allantoin: Allantoin is one of the well-known azaheterocycles in the imidazolidinone series, specifically the hydantoins. Several generalizing communications have been written about its beneficial biological characteristics. is renowned for its calming, hydrating, and skin-enhancing attributes. It is frequently integrated into skincare and cosmetic items. The fundamental process through which allantoin operates predominantly centers on its impact on skin cells and tissues on the other hand, to yet, there are no studies in the literature that illustrate the allantoin's generalized chemistry. Based on the aforementioned, this study intends to increase the potential for application of allantoin-based compounds in organic synthesis and daily life by bringing to the attention of chemists and experts in related disciplines the processes for preparing allantoin as well as its chemical features. Allantoin is a skin-active component that has keratolytic,

moisturizing, calming, and anti-irritant qualities. It also promotes epidermal cell renewal and hastens the healing of wounds. Allantoin has a high level of skin and cosmetic raw material compatibility, is risk-free, and is not irritating. Allantoin has a long history of use in topical medications and cosmetics without any reports of toxicity or negative side effects. Observe the JSCI and CTFA requirements. Allantoin is a substance that is endogenous to the human body and also found as a normal component of human diets. In healthy human volunteers, the mean plasma concentration of allantoin is about 2-3 mg/l. During exercise, the plasma allantoin concentration rapidly increases about two fold and remains elevated. In human muscle, urate is oxidized to allantoin during such exercise. The concentration of allantoin in muscles increases from a resting value of about 5000 ug/kg to about 16000 ug/kg immediately after short-term exhaustive cycling exercise. More specifically, allantoin is a diureide of glyoxylic acid that is produced from uric acid. It is a major metabolic intermediate in most organisms. Allantoin is found in OTC cosmetic products and other commercial products such as oral hygiene products, in shampoos, lipsticks, anti-acne products, sun care products, and clarifying lotions.

Structure: -

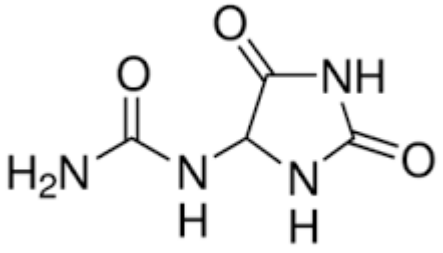

Figure 1.1 Chemical Structure of Allantoin

Molecular Formula: $C_4H_6N_4O_3$

Molecular Weight: 158.12 g/mol

Mechanism of Action: Allantoin operates by influencing skin cells and tissues, delivering advantages such as stimulating skin cell growth and rejuvenation. This is valuable for aiding wound healing and tissue repair. Furthermore, allantoin possesses a mild exfoliating impact, gently smoothing the skin's surface by eliminating dead cells. Its capacity to moisturize aids in retaining skin moisture, particularly beneficial for those with dry or sensitive skin. Additionally, allantoin is recognized for its capability to alleviate irritation and inflammation, making it appropriate for calming sensitive skin. When combined with other active substances, it also heightens the absorption of these compounds. Overall, the multifaceted effects of allantoin work together to enhance skin well-being and appearance However, continuing research indicates that allantoin may generate a histological wound healing profile in rats that improves and speeds up the restoration of normal skin. In contrast to rat subjects with wounds that did not receive any allantoin administration, wounds inflicted on those subjects histologically showed increased vasodilation, the

presence of inflammatory exudates, the number of inflammatory cells, angiogenesis, fibroblast proliferation, and increased collagen deposition.

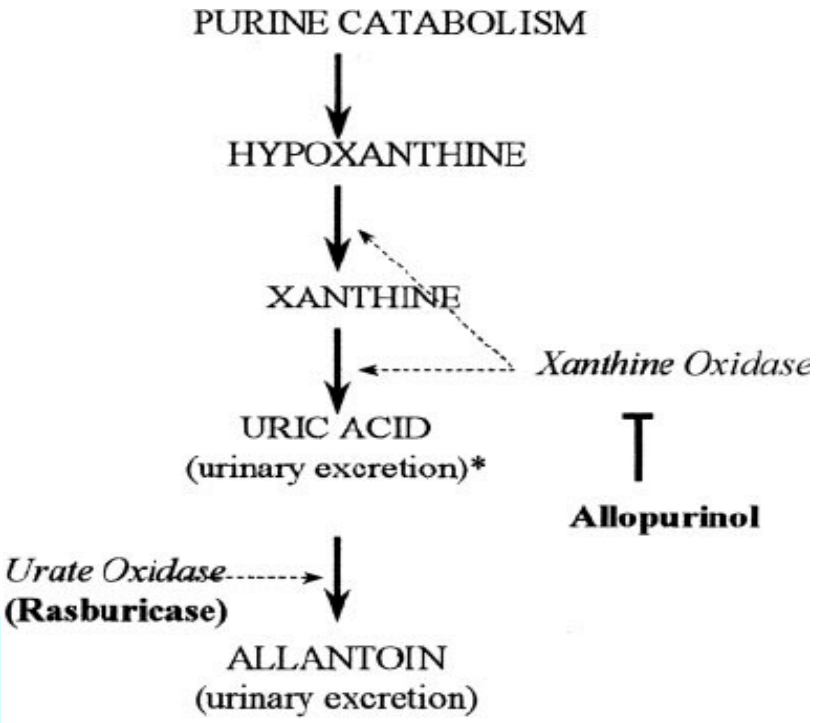

Figure 1.2 Mechanism of Action of Allantoin

Description: Allantoin is an imidazolidine-2,4-dione that is 5-aminohydantoin in which a carbamoyl group is attached to the exocyclic nitrogen. It has a role as a vulnerary, a human metabolite, a Saccharomyces cerevisiae metabolite and an Escherichia coli metabolite. It is a member of urea's and an imidazolidine-2,4-dione. It is functionally related to a hydantoin. It is a tautomer of a 1-(5-hydroxy-2-oxo-2,3-dihydroimidazol-4-yl) urea.

Figure 1.3 Allantoin

Mode of Action: Allantoin has been shown to have favorable benefits on skin. Allantoin is a moderate keratolytic agent that aids in the natural desquamation of stratum corneum and improves skin smoothness by dissolving the intercellular cement that keeps the cornified cells together. The capacity to increase the amount of water attached to the keratin and intercellular matrix results in the moisturizing effect, which

softens the skin and makes it appear healthier. The ability of allantoin to form complexes and neutralize numerous irritating and sensitizing chemicals is what gives it its calming, anti-irritant, and skin-protective effects. Allantoin boosts damaged epithelium's regeneration, speeds up wound healing, and increases epidermal cell proliferation.

Origin: Allantoin is a metabolic intermediate found in many different types of organisms, including bacteria, plants, and animals. Numerous plants contain allantoin, but the leaves and roots of the herb comfrey (Symphytum officinale), a member of the Boraginaceae family, are particularly rich sources. This herb's roots and leaves, which can be used to make poultices and decoctions to cure wounds, have a long history of use. They contain between 0.6 and 1% allantoin. In mammals (apart from primates), allantoin is the byproduct of purine breakdown and results from the oxidation of uric acid

Pharmacology and Biochemistry: The pharmacodynamic effects of allantoin cannot be explicitly supported by well-controlled and suitable data. However, ongoing research indicates that allantoin has moisturizing and keratolytic properties, as well as the capacity to raise the extracellular matrix's water content and improve the desquamation of the upper layers of dead skin cells—all of which are processes that can encourage cell division and speed wound healing. In skincare products, synthetic allantoin is frequently employed owing to its dependable quality and ready availability.

Pharmacokinetic Properties:

Absorption: In studies on human subjects, a recovery of 19% and 34% of allantoin in the urine was observed but only in two individuals and only after the administration of massive doses of allantoin. After intravenous administration, recovery in the urine was practically quantitative with doses of 75 to 600 mgm in the human model. After 240 mgm, excretion continued for 72 hours in human subjects and the results were similar in regards to subcutaneous injection.

Distribution: The amount of allantoin discharged in the urine after being given to dogs orally as a solid or solution ranged from 35 to 92 percent in just 24 hours. When given orally to rabbits, no allantoin was found in either the urine or the faces. In two human subjects after receiving high dosages, recovery rates were 19 and 34%. Recovery in the urine after intravenous injection was essentially quantitative in both the dog and the human, with dosages ranging from 75 to 600 mg. 72 hours passed following 240 mg in a man's urine

Metabolism: The enzyme known as uricase has the ability to change uric acid into allantoin. Uric acid is the only final breakdown product in the purine degradation of undesired waste product purine nucleotides since humans lack endogenous uricase. Allantoin is consequently produced by non-enzymatic reactions between reactive oxygen species and uric acid in human urine. As a result, such non-enzymatic activities are

potentially appropriate indicators for detecting oxidative stress in ageing and chronic disorders.

Properties and Stability: A heterocyclic substance produced from purine is allantoin. It is an odourless, white powder that dissolves in water up to 5%, dissolves in alcohols only very slightly, and is insoluble in oils and a polar solvent. In the pH range of 3 to 8, and after extended heating to 80°C, allantoin is stable. It is completely compatible with cationic, anionic, and non-ionic systems as well as cosmetic components.

Applications:

Any application of personal care can benefit from allantoin. Every cosmetic preparation performs better when it is used, giving intact skin a smooth, healthy appearance at low doses and providing pain relief and healing for skin that is irritated, chapped, or cracked at high doses. As the only active component, allantoin is also helpful.

Among the various cosmetic uses are:

- Body and face care: tonics, gels, creams, lotions, wipes.
- Hand-care: gels, lotions, creams.
- Shaving-care: shaving soaps, aftershaves, gels, lotions, creams.
- Baby-care: diaper rash, bath products, gels, lotions, creams, powders, wipes.
- Lips-care: sticks, creams.
- Sun-care: sunscreens, after suns, suntans, gels, lotions, creams.
- Hair products: shampoos, tonics.
- Bath products: shower gels, bubble baths, intimate, powders, wipes.
- Oral preparations: toothpastes, mouthwashes.

MATERIALS AND METHODS

Material: We bought allantoin and choline chloride from Sigma-Aldrich in purity levels of 98%. Alfa Aesar's anhydrous zinc chloride had a purity of more than 98%. We purchased high-purity chromatography solvents from Alfa-Aesar or Sigma-Aldrich. All aqueous preparations were made with ultrapure water from Millipore's Milli-Q Advantage A10 System in France.

Synthesis of Hydrogels:

Three different hydrogel samples were created by dispersing 5% (w/v) allantoin in deionized water at 80°C in a water bath with constant stirring until dissolved. The three solutions were then chilled to room temperature, and various 5%, 10%, and 20% (w/v) quantities of lyophilized Aloe vera powder were

gradually Salicylic acid, at a concentration of 1% (w/v), was then added. The mixtures were agitated for 6 hours or so are needed for homogenous mixing. The outcome of adding 2% (w/v) xanthan gum each of the three hydrogels quickly gels. Three homogeneous composite hydrogels round out the list. utilizing a three-dimensional mould, with various Aloe vera concentrations. structure with the designations.

Characterization Method

Visual Examination

In terms of specific organoleptic features including appearance, consistency, colour, homogeneity, and the presence of any agglomerations or phase separation, the three composite hydrogel formulations made with various quantities of aloe vera were assessed. allantoin typically appears as a colorless crystalline powder with no scent, and it easily dissolves in water.

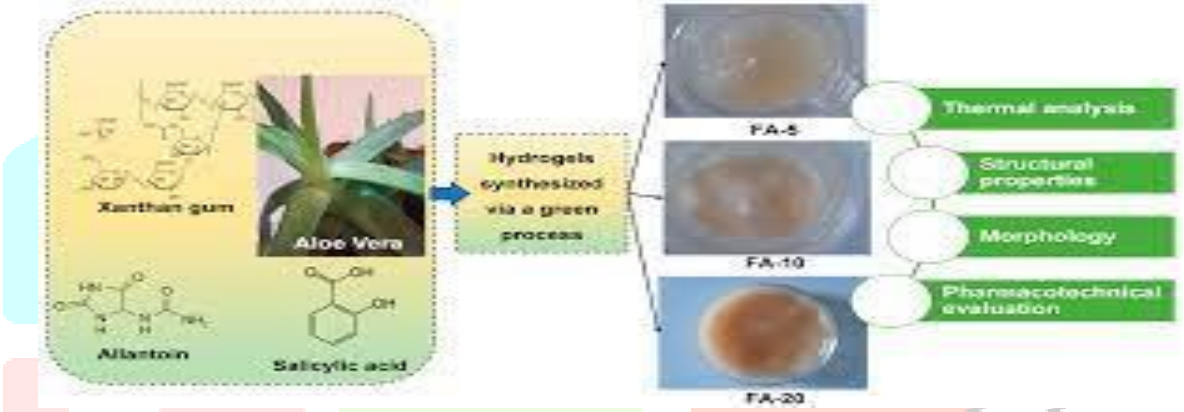

Figure 2.1 Scheme of synthesis, optical image of three composite hydrogel with different Aleo Vera concentration (FA-5, FA-10, and FA-20) and their concentration.

Methods:

Using an Agilent4100Ex-oScan Spectrometer (Santa Clara, CA, USA) diffuse external reflectance system at the sample surfaces, between 400 and 4000 cm 1, with a resolution of 4 cm 1 and a measurement duration of 15 s, Fourier transform infrared FTIR spectrum measurements were made. Using a analytical Empyrean diffractive, X-ray diffraction spectra (XRD) were acquired at room temperature. With an anti-scatter slit attached on the PIXcel3D detector on the diffracted side and a programmable divergent slit on the incident side, the diffractometer was operated with in-line focusing. A Cu X-ray tube (Cu K1 = 1.541874) was used to capture XRD diffraction patterns in a Bragg-Brentano geometry from 20 to 80 ter at a scan step of 0.02 and a measuring time step of 2 s. Using a Mettler Toledo, differential scanning calorimetry (DSC) analysis was captured. DSC 3 calorimeter employing nitrogen gas from Mettler-Toledo GmbH in Greifensee, Switzerland 80 mL per minute flow in crimped aluminium pans with punctured lids. TG: thermoradiometer Using a Mettler Toledo, analysis and differential thermal gravimetry (DTG) were carried out.

Pharmacotechnical Evaluation:

Tensile Strength and Elongation Ability Using a digital tensile force tester for universal materials (Lloyd Instruments Ltd., LR 10K Plus, West Sussex, UK), the mechanical characteristics of the dry hydrogels were assessed. Measurements were taken at a distance of 30 mm and a speed of 30 mm/min. Between the two plates, the hydrogel was placed vertically, and the breakage force was measured. The tests were run three times, and the mechanical characteristics were computed using the formulas below:

Tensile strength (kg/mm2) = Force (kg) at break.

Film width (mm) Film thickness (mm)

Elongation (%) = Extended length of the film

Initial running time: 100 (2)

Moisture Content:

The moisture content was measured using an HR 73 Mettler Toledo halogen humidity analyzer from Mettler-Toledo GmbH, Greifensee, Switzerland, using the thermogravimetric technique. The loss on drying (%) was calculated using dry composite hydrogels.

pH Analysis:

A CONSORT P601 pH-meter was used to measure the pHs of the synthetic composite hydrogels. The wet and dry hydrogel samples were moistened for 5 min at room temperature using 1 mL of distilled water with a pH of 6.5 0.5. For each series, measurements are conducted for five experiments, and pH values are reported.

Swelling Ratio:

Dry samples that were precisely weighed were fixed on 1.5% agar gel in Petri plates and incubated at 37°C. Every 30 minutes for 6 hours, the samples were weighed once again. Equation (3) was used to calculate the swelling ratio.

Swelling ratio (%) = Wt-Wi/Wi X 100

Where, Wi is the starting weight and Wt is the sample weight at time t following incubation.

Spreadability:

Gels' essential property of spread ability connects their rheological and structural features. It is a useful test for assessing semi-solid topical formulations since it can reliably anticipate behavior during product application and removal. Wet hydrogels were subjected to a spread ability examination using the extensiometric approach, which looks at how easily they can deform in response to applied weights. There were two 20 cm by 165 g square glass plates utilized. We put the second glass plate and gently pressed it onto the lower plate after placing 1 g of each sample on it. The gel circle's diameter was measured after one minute had passed. Weights of 50, 100, 200, and 500 g were successively added to the extensometer’s top plate at intervals of one minute. The sizes of the circles formed by sample spreading were recorded for each.

Physical and Chemical Characteristics:

Allantoin is a colorless powder with no scent or flavor, and it does not cause stains. It is considered an amphoteric substance. The chemical attributes of allantoin are detailed in Table 2. Akema Fine Chemicals mentioned that allantoin exists in solution in an equilibrium mixture of ketonic and enolic forms. With a single chiral center, the enantiomers R and S are present in equal proportions, rendering the mixture optically inactive. Extraction methods can yield optically active versions. Allantoin dissolves in hot water, has limited solubility in cold water, glycerin, and propylene glycol, slight solubility in alcohol, and is almost insoluble in nonpolar solvents like mineral oil, dimethylisosorbide, ether, and chloroform. Allantoin ascorbate is a white-yellowish powder that is soluble in water.

Stability:

Allantoin undergoes degradation when it is dissolved in distilled water. At a concentration of 0.13% allantoin (0.6556 g in 500 mL), 6.3% of the compound degraded after 620 days. When the concentration was 0.45% (1.1396 g in 250 mL), 1.5% degraded after 415 days. Similarly, at a concentration of 0.24% (2.421 g in 1000 mL), 6.4% degraded after 24 days. When 0.13% allantoin was dissolved in tap water, 6.4% degraded after 24 days. When two samples of allantoin (25 mL each) were mixed with 23.94 mL of potassium hydroxide (KOH) and left for a month, there was a 90.2% and a 91.1% degradation respectively. Another experiment involved incubating two samples of allantoin (25 mL each) in KOH (20 mL) for 24 hours at body temperature, resulting in a 43.4% degradation of allantoin. Kaliszan and Halkiewicz utilized infrared analysis to detect degradation in stored allantoin

CONCLUSION AND DISCUSSION

A smooth texture and a range of beige hues, from light transparent to deep opaque, could be found in the freshly made composite hydrogels (Figure 1). According to the specialised literature [32,33,41], Table 1 displays the organoleptic characteristics of hydrogel composites with varying Aloe vera concentration. The hydrogels' homogenous and constant microstructure was revealed by optical and SEM examinations. As shown in Section 3.8 below (at least three measurements were utilised for the mean and SD values), the hydrogels also exhibited consistent swelling, elasticity, and mechanical strength behavior.

FTIR Spectroscopy:

Figure 2 displays the FTIR spectra of the hydrogels made from Aloe vera.

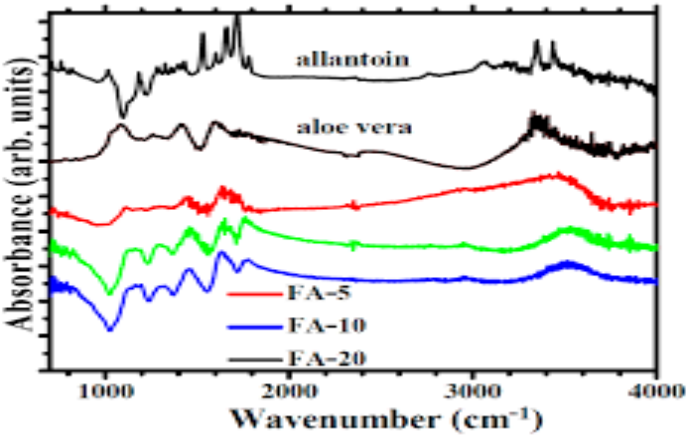

Figure 3.1 FTIR spectra of the raw material and three formulation of aleo vera based hydrogels(FA-5, FA-10 and FA-20).

Based on the outcomes, the FTIR spectrum interpretation was completed. and by comparison with the information provided for various types of dry Aloe vera dried hydrogels in literature. Note that the FTIR study only considers the surface. enables the identification of the so-called short-range order at the level of the sample and atomic level. Similar characteristics can be seen in the spectra of the three FA materials (Figure 2, FA-5, FA-10, and FA-20), with the strength of the vibrational bands being lowered for the composition containing the least quantity of Aloe vera. Despite the higher Aloe vera content, no discernible alterations were identified between the FTIR spectra of FA-10 and FA-20. atomic level. The spectra revealed six major functional groups with centres at 3453, 1741, 1633, 1427, 1290, and 1170 cm1. Additionally, two weak bands at 2925 and 2755 cm1 have been found.

In Figure 3.1, the FTIR spectra of the aloe vera precursor and allantoin are also displayed for comparison. We mostly saw the stretching vibrations of the vOH and CH2 atoms in the 4000–2800 cm–1 spectrum region. A wide band with a centre of 3453 cm1 exists between 3600 and 3200 cm1.

The uronic acid, mannonse, galacturonic acid, and phenolic -OH stretching groups in the carbohydrate monomers from Aloe vera are responsible for this band.components of antraquinones, such as aloin and emodin), in accordance with earlier observations. A wide range like this might also point to the occurrence of intermolecular hydrogen bonds brought on by dipole-dipole attraction forces. It is still very challenging to establish a sensible connection between these strong OH stretching bands and particular vibrational states. According to data from the prior literature, the broad OH stretching band is attributed to the contribution of different vibrational states of the intricate web of inter- and intramolecular hydrogen bonds present in the polysaccharide structure, particularly the carbohydrate monomers of Aloe vera (uronic acid, galacturonic acid, and phenolic compounds). Both the asymmetric (2958 cm1) and symmetric (2755 cm1) C-H group stretching vibrations are linked to low-intensity bands in the 2800–3000 cm1 range. The polysaccharides from Aloe vera cause two band vibrations, centred at 1760 cm1 and 1433 cm1, which are indicative of carbonyl stretching and correspond to the asymmetrical and symmetrical -COO- of carboxylic acid (-COOH) groups. These band vibrations have also been observed in other reported data. The C=O stretching of the carboxylic ester group—COOCH3—causes the high-intensity mode band visible at approximately 1633 cm1; this finding is consistent with earlier reports of observations. These functional groups have a

connection to pectic chemicals, polysaccharides, and water, which are the main constituents of gels made from Aloe vera. In vegetative tissues, polysaccharides are the most prevalent substance. In general, they can be classified into storage polysaccharides like acemannan, the primary bioactive component in the case of Aloe vera, and cell wall polysaccharides like cellulose, hemicelluloses, and pectins. The desire for high polysaccharide content in commercial Aloe vera products is the main driver behind the extensive research on the effects of drying processes, including preparation method, temperature, pH, O2, and the presence of other compounds, as well as polysaccharides and their chemical and biological characteristics, such as chain length, monosaccharide composition, emulsifying activity, and structural conformation.

XRD Analysis:

In order to better understand the structure of hydrogels made from Aloe vera, XRD analysis was used. in the Supplementary Information displays the XRD patterns of the three composite Aloe vera-based hydrogels, allantoin, and xanthan gum.

Resources File. The allantoin XRD spectrum (Figure S1a in the Supplementary Materials

At 2 = 15.9, File) has strong diffraction peaks.

20.5◦, 22.2◦, 24.7◦, 28.2◦, 29.8◦, 32.17◦,and 35.1◦, confirming its crystalline structure and in conformity with research data.

Both xanthan gum (Figure S1a in the Supplementary Materials File) and aloe vera powder have amorphous XRD patterns that do not exhibit sharp peaks. This is consistent with other researchers' reports on the amorphous form of xanthan gum and aloe vera.

Raman Analysis

The dried gel was subjected to raman spectroscopy analysis to determine the presence of various functional groups and forms of bonding in each gel and compare their spectra. The Raman spectra of the FA materials and Aloe vera precursor powder are displayed in Figure 3.

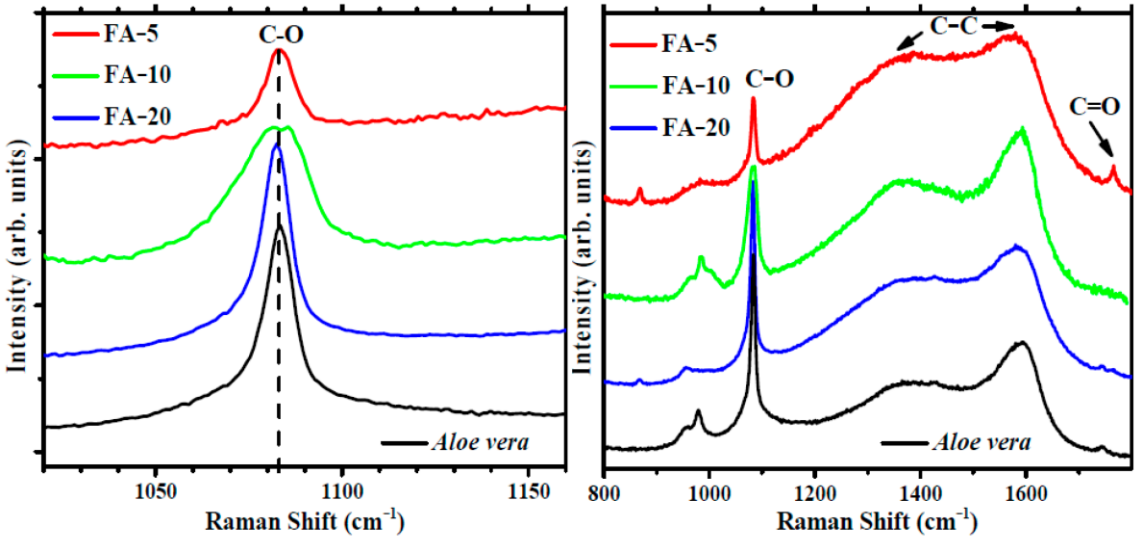

(a) (b)

Figure 3.2 Raman spectra of FA-5 (red line), FA-10 (green line), FA-20(blue line) and Aloe Vera (a) and detail of the spectra in the region of the main characteristics band of acemannan (b).

A prominent peak at 1083 cm1 dominates the spectra. The acemannan chain's C-O stretching vibrations are represented by this band [46]. One of the key bioactive components and the main long-chain polysaccharide (carbohydrate) present in aloe vera leaf gel is acemannan. With increasing Aloe vera content, the relative intensity of the acemannan vibrational mode also rises, whereas FA-5 and FA-20 exhibit a dramatic peak width at half peak of 10 cm1 that is comparable to that observed on the Aloe vera precursor. FA-10 has a modal width at half peak of 25 cm1, which is wider. cause two band vibrations, centred at 1760 cm1 and 1433 cm1, which are indicative of carbonyl stretching and correspond to the asymmetrical and symmetrical -COO- of carboxylic acid (-COOH) groups. These band vibrations have also been observed in other reported data of this raman analysis.

DSC Analysis: Figure 4 displays the DSC curves for samples containing various amounts of aloe vera.

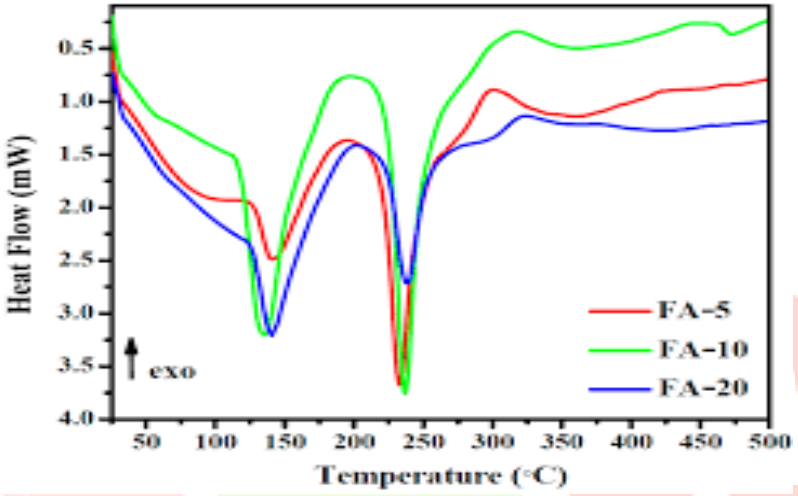

Figure 3.3 DSC Curve of hydrogels containing 5,10, and 20% (w/v) aloe vera.

The sublimation of salicylic acid, which happens below 100 °C, does not show a clear peak. The volatile fraction, primarily water coupled to the structure, vaporises at a significant endothermic peak about 140 ° according to the DSC curves. The TGA curves presented below in section 3.5 evaluate this thermal event as well. At about 230 °C, a second endothermic reaction in DSC is clearly seen for all samples and is connected to the thermal breakdown of the polymeric component. While Garcia Orue confirmed the existence of two endothermic peaks at 68 and 156 °, Yoshida et al. identified two main endothermic peaks for Aloe vera extract at about 84.59 °C and 214.9 °.

Thermal Analysis:

The TG/DTG curves obtained for each of the three Aloe vera-based hydrogels are displayed in Figures 5a through 5c, while the TG curves are shown collectively in Figure 5d for comparison.

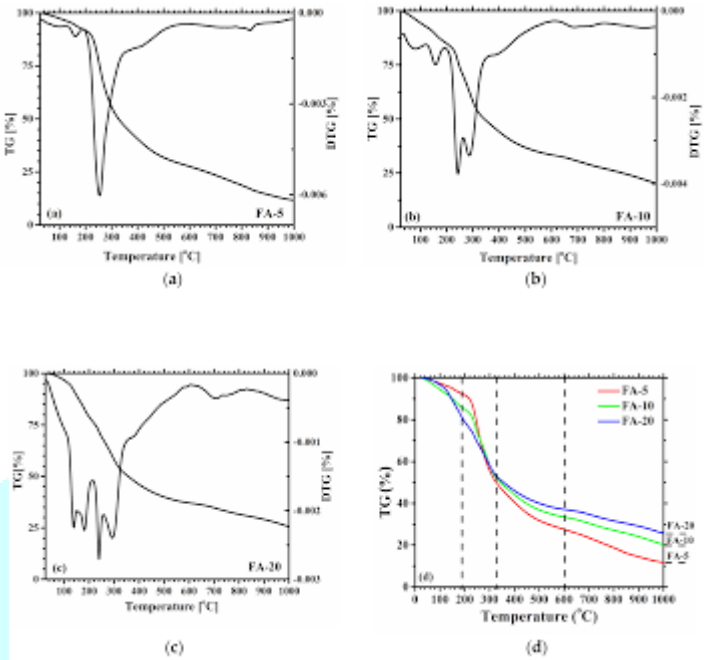

Figure 3.4 The TG/DTG curve for the three Aloe vera based Hydrogels (a) FA-5, (b) FA-10, (c) FA-20, (d) Comparison of the TG behaviors.

Because combined with DSC analysis, these two techniques aid in understanding the physical and chemical interactions of the compounds, thermogravimetric analysis was carried out to assess the thermal stability of the samples. It is clear that all hydrogels exhibit multiple-stage thermal degradation and similar TG curves, with the majority of weight loss taking place between 200 and 300 C. The main variations may be seen in the relative strength of the thermal effects that are seen along with weight loss in the DTG curves, which are particularly noticeable in the sample with the highest Aloe vera content. A wider range of thermal decomposition temperatures was produced by the gels' slightly altered thermal behaviour brought about by their increased Aloe vera content. The TG/DTG curves exhibit four distinct stages of heat degradation, which are represented in Figure 5d by dashed lines for visual guidance

SEM Analysis

All dried gels condensed into homogeneous polymeric solids, according to a SEM morphological analysis At the microscale, the gels' structure was consistent, and the components of the hydrogel were distributed evenly. The surfaces of all three materials are comparatively dense. The higher-magnification micrographs of FA-5 show sub-micron sized holes.

AFM Result

The surface topography at the nanoscale was determined using AFM. From color-enhanced AFM images captured in topographic mode, Figure 6 shows AFM pictures and line profiles of samples FA-5, FA-10, and FA-20 at the (8 m 8 m) scale. The FA-5 sample is smoother than the FA-10 sample and exhibits a pattern of

random shallow poresshowing that the morphology of the Aloe vera based hydrogel samples is largely dependent on their composition (Aloe content). These pores in sample FA-5 are several hundred nanometers in diameter but just tens of nanometers deep. The cross-sectional height profiles of sample FA-5 have a corrugated shape due to the texture, which is made up of tiny particles that are grouped singly or in groups and give the illusion of being nanometer-sized fibrils. such as the 400 nm-diameter one indicated along the green line. Compared to the FA-10 sample, the FA-5 sample is smoother and reveals a structure of sporadic shallow pores. However, the two samples'. For example, sample FA-5's two line-scans' z-scales are about 30–40 nm high (40 nm at the red line, from 30–+10 nm, and 30 nm at the green line, from 20–+10 nm), whereas sample FA-10's two line-scans' z-scales are about 100–nm high. The FA-5 sample has a peak-to-valley level difference of 63.8 nm and an RMS roughness of 6.5 nm for all scanned areas, while the FA-10 sample has a peak-to-valley parameter of 232.7 nm and an RMS roughness of 36.1 nm. The surface morphology is completely altered by further modifying the sample composition, and displaying a "dense" structure of nanometer-sized surface pores. These pores, which are depicted in Figure 6c as tiny pits (black dots), range in size from tens to hundreds of nm (the largest), with a few nm serving as their depth. For instance, the pore in Figure 6c with two red arrows along the green line-scan has a depth of 3 nm and a diameter of 120 nm. The FA-20 sample exhibits an RMS roughness of 2.1 nm and a peak-to-valley level difference of 17.5 nm for the whole (8 m 8 m) scanned area in Figure 6c.

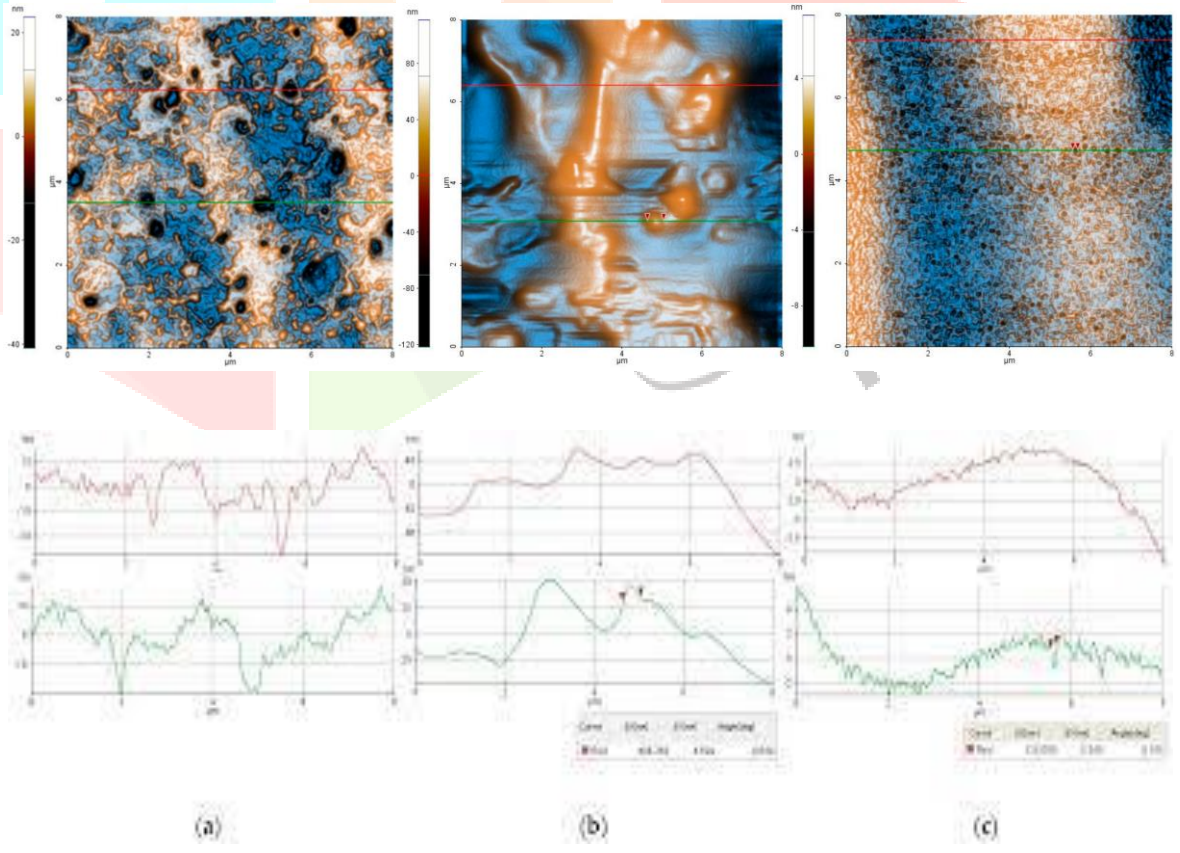

Figure 3.5 Enhanced color 2D AFM images at the scale of (8 um X 8um), together with representative line scan for the

REFERENCE:

1. MacCarthy-Morrogh, L. and Martin, P., 2020. The hallmarks of cancer are also the hallmarks of wound healing. *Science signaling*, *13*(648), p.eaay8690
2. Sheker, K.M., Black, H.J. and Lach, J.L., 1972. Silver allantoinate for the topical treatment of burns. *American Journal of Health-System Pharmacy*, *29*(10), pp.852-855.
3. Mecca, S.B., 1976. URIC ACID, ALLANTOIN AND ALLANTOIN DERIVATIVES.
4. MacCarthy-Morrogh, L. and Martin, P., 2020. The hallmarks of cancer are also the hallmarks of wound healing. *Science signaling*, *13*(648), p.eaay8690.
5. IONIȚĂ, F., COMAN, C. and CODREANU, M., 2022. THE RAT AS AN ANIMAL MODEL FOR THE EVALUATION OF THE CUTANEOUS WOUND HEALING. *Scientific Works. Series C, Veterinary Medicine*, *68*
6. Agnes, C.J., Murshed, M., Takada, A., Willie, B.M. and Tabrizian, M., 2023. A 6-bromoindirubin-3′-oxime incorporated chitosan-based hydrogel scaffold for potential osteogenic differentiation: Investigation of material properties in vitro. *International Journal of Biological Macromolecules*, *227*, pp.71-82.
7. Pounikar, Y.O.G.E.S.H., Jain, P.U.S.H.P.E.N.D.R.A., Khurana, N.A.V.N.E.E.T., Omray, L.K., Patil, S. and Gajbhiye, A., 2012. Formulation and characterization of Aloe vera cosmetic herbal hydrogel. *International Journal of Pharmacy and Pharmaceutical Sciences*, *4*(4), pp.85-86.
8. Pounikar, Y.O.G.E.S.H., Jain, P.U.S.H.P.E.N.D.R.A., Khurana, N.A.V.N.E.E.T., Omray, L.K., Patil, S. and Gajbhiye, A., 2012. Formulation and characterization of Aloe vera cosmetic herbal hydrogel. *International Journal of Pharmacy and Pharmaceutical Sciences*, *4*(4), pp.85-86.
9. Becker, L.C., Bergfeld, W.F., Belsito, D.V., Klaassen, C.D., Marks, J.G., Shank, R.C., Slaga, T.J., Snyder, P.W. and Andersen, F.A., 2010. Final report of the safety assessment of allantoin and its related complexes. *International journal of toxicology*, *29*(3_suppl), pp.84S-97S.
10. BRITTO, M.D.R.S., 2017. *Desenvolvimento e validação de metodologias analíticas para o controle de qualidade da droga vegetal e produtos derivados de Symphytum officinale L.(confrei)* (Master's thesis, Universidade Federal de Pernambuco)